Available online at www.sciencedirect.com
ScienceDirect
Biochimica et Biophysica Acta 1778 (2008) 185–197
Biochimica et Biophysica Acta
BBA
www.elsevier.com/locate/bbamem

Sphingomyelinase generation of ceramide promotes clustering of nanoscale domains in supported bilayer membranes

Ira, Linda J. Johnston *

Steacie Institute for Molecular Sciences, National Research Council Canada, Ottawa, ON, Canada K1A 0R6

Received 16 July 2007; received in revised form 20 September 2007; accepted 21 September 2007
Available online 4 October 2007

Abstract

The effects of ceramide incorporation in supported bilayers prepared from ternary lipid mixtures which have small nanoscale domains have been examined using atomic force and fluorescence microscopy. Both direct ceramide incorporation in vesicles used to prepare the supported bilayers and enzymatic hydrolysis of SM by sphingomyelinase were compared for membranes prepared from 5:5:1 DOPC/sphingomyelin/cholesterol mixtures. Both methods of ceramide incorporation resulted in enlargement of the initial small ordered domains. However, enzymatic ceramide generation led to a much more pronounced restructuring of the bilayer to give large clusters of domains with adjacent areas of a lower phase. The individual domains were heterogeneous with two distinct heights, the highest of which is assigned to a ceramide-rich phase which is hypothesized to occur via ceramide flip-flop to the lower leaflet with formation of a raised domain due to negative membrane curvature. A combination of AFM and fluorescence showed that the bilayer restructuring starts rapidly after enzyme addition, with formation of large clusters of domains at sites of high enzyme activity. The clustering of domains is accompanied by redistribution of fluid phase to the periphery of the domain clusters and there is a continued slow evolution of the bilayer over a period of an hour or more after the enzyme is removed. The relevance of the observed clustering of small nanoscale domains to the postulated coalescence of raft domains to form large signaling platforms is discussed.

Keywords: Atomic force microscopy; Bilayer; Ceramide; Membrane; Total internal reflection fluorescence

1. Introduction

Membrane compartmentalization into sphingolipid- and cholesterol-rich lipid rafts has been implicated in a wide range of biological process including signal transduction, lipid trafficking and viral and bacterial entry [1–5]. Sphingomyelin is the most abundant sphingolipid and recently the role of ceramide – a sphingomyelin metabolite – in modulating raft structure and function has received special attention. Ceramide is a well-known bio-active lipid involved in various cell signaling pathways [6–8]. It is thought to be a second messenger in a variety of cellular processes such as apoptosis, senescence, bacterial pathogenesis and cell cycle arrest. Some studies have suggested that ceramide acts as a second messenger by binding to specific intracellular protein targets. However, other studies have concluded that its function as a signaling molecule is mediated through its strong impact on membrane structure, for example by induction of membrane heterogeneity through formation of ceramide-rich domains and/or nonlamellar structures and membrane vesiculation and fusion.

Ceramide can be generated de novo in the cell or through hydrolysis of sphingomyelin (SM) by signal-activated sphingomyelinases (SMase) in membranes [9]. Hydrolysis of raft-sphingomyelin is thought to drive coalescence of small raft domains into large platforms, providing sites for oligomerization of cell-surface receptors as well as internalization of bacteria and to aid in the inhibition of HIV invasion of cells [8,10]. Indeed, in cellular systems the activation of SMase has been correlated to formation of large patches as visualized by raft-markers.

Abbreviations: AFM, atomic force microscopy; chol, cholesterol; DOPC, 1,2-dioleoyl-*sn*-glycero-3-phosphocholine; DPPC, 1,2-dipalmitoyl-*sn*-glycero-3-phosphocholine; ESM, egg sphingomyelin; GUV, giant unilamellar vesicles; PC, phosphatidylcholine; SMase, sphingomyelinase; TIRF, total internal reflection fluorescence; TR-DHPE, Texas Red® 1,2-dihexadecanoyl-sn-glycero-3-phosphoethanolamine, triethylammonium salt

* Corresponding author.
E-mail address: Linda.Johnston@nrc-cnrc.gc.ca (L.J. Johnston).

0005-2736/$ - see front matter.
doi:10.1016/j.bbamem.2007.09.021

The impact of ceramide on cell membranes can be explained on the basis of its structure and physical properties [7]. Ceramides are sphingolipids with a sphingosine base linked via its amino group to a fatty acid chain and are among the least polar and most hydrophobic lipids in membranes. They have small polar headgroups that result in a negative membrane curvature, are extensively hydrogen bonded since the polar head group can act both as a hydrogen bond acceptor and donor and have high melting temperatures. These properties explain a number of the effects of ceramide on model membranes, including their ability to increase lipid order, form ceramide-rich domains, promote the formation of non-lamellar structures [11,12] and induce transbilayer flip-flop [11,13,14]. Another interesting property of ceramide is its effect on cholesterol (chol)-rich liquid-ordered phases. It has been hypothesized that ceramide displaces cholesterol from rafts in model [15–18] and cellular membranes [19] and experiments using ceramide/chol/phosphatidylcholine (PC) mixtures indicate that this displacement follows a 1:1 relationship [18].

The complexity of cell membranes has made it important to study the effect of ceramide on simpler model membranes. For example, treating PC/SM giant vesicles with SMase led to formation of ceramide patches that coalesced into ceramide-rich macrodomains and then formed vesicles [20,21]. Ceramide platform formation has also been observed in fluid phospholipid vesicles [22] and ceramide-enriched domains have been visualized directly by fluorescence microscopy in SM/ceramide GUVs [23]. We have recently shown that enzymatic generation of ceramide in model raft membranes results in large scale membrane restructuring [24]. Upon ceramide generation in micron-sized SM- and chol-rich rafts, large heterogeneous domain clusters were observed along with smaller heterogeneous domains and areas devoid of domains. This work and related studies [17,25,26] provide evidence for ceramide-rich ordered domains that coexist with a mixture of liquid-ordered and liquid-disordered phases.

Despite the detailed characterization of ceramide-enriched domains in various model systems, the direct visualization of the effect of ceramide on small nanoscale ordered domains that are more relevant to rafts in cellular membranes has yet to be studied. We have extended our previous study to examine the direct and enzymatic incorporation of ceramide in DOPC/SM/chol mixtures that form nanoscale domains — similar in size to rafts *in vivo* [27]. We use a combination of atomic force microscopy (AFM) and total internal reflection fluorescence (TIRF) imaging to probe the morphology of ceramide containing bilayers. The utility of AFM for studies of the nanoscale organization of model raft membranes under physiological conditions in aqueous solution has been well demonstrated [28–32]. Fluorescence imaging, on the other hand, provides better time resolution and allows for repeated imaging of the same area, unlike AFM where tip contamination often makes this difficult [33]. We show that direct incorporation of ceramide leads to enlargement of the small domains formed in DOPC/egg SM/chol bilayers. Enzymatic ceramide generation, on the other hand, leads to fast (minutes time scale) membrane re-structuring that includes increases in size as well as heterogeneity and clustering of domains. The relevance of these results to ceramide induced raft coalescence in cell membranes is discussed.

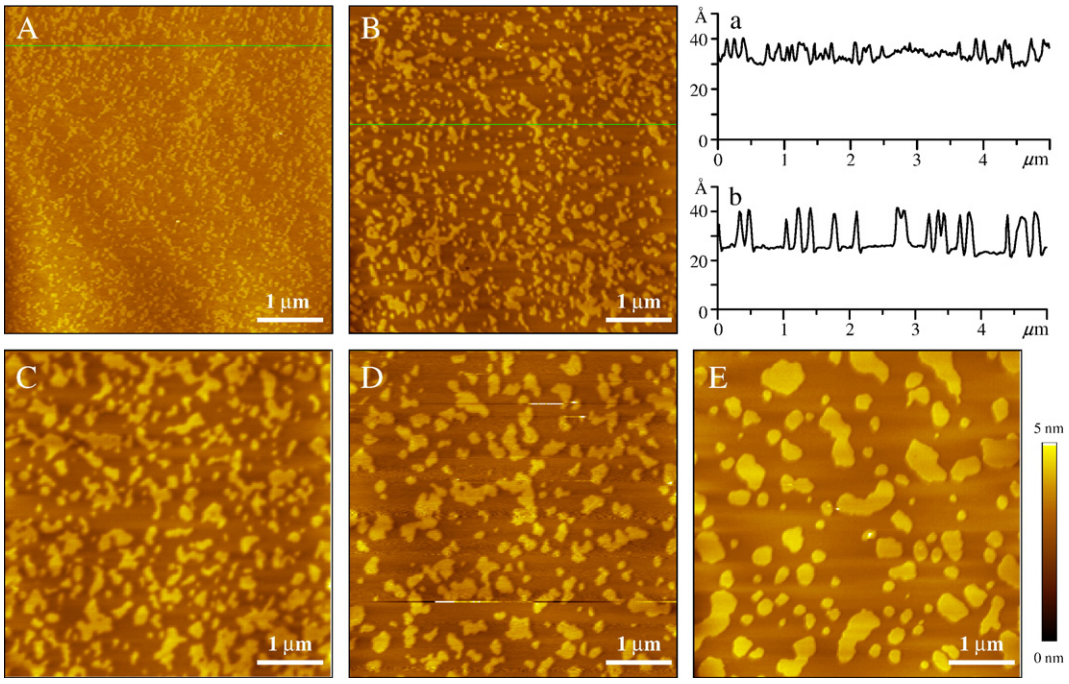

Fig. 1. DEC 551 bilayers imaged (A) 45 min and (B) 3 h after bilayer formation. Cross sections for the lines indicated in images A and B are shown in a and b and the z-scale is indicated in the color bar. The domain size increases and the height difference between domain and the surrounding lower phase increases from 10.5 Å to 14.1 Å in the first 3 h after bilayer formation but remains stable thereafter. Bilayers with increasing ceramide (Cer) concentration at a constant sphingomyelin (SM) plus Cer content of 45.5%: (C) 1.8%, (D) 4.5% and (C) 9.1% Cer. The domain size increases with the addition of Cer while the domain height (see Fig. 2) decreases slightly.

2. Materials and methods

2.1. Materials

DOPC, egg SM (ESM), $C_{16:0}$ ceramide and cholesterol were obtained from Avanti Polar Lipids and were used as received. Sphingomyelinases (SMase) isolated from *Bacillus cereus* and *Staphylococcus aureus* were from Sigma-Aldrich. For SMase activity, 1 U is defined as the amount of enzyme that will hydrolyze 1.0 μmol of TNPAL-sphingomyelin per min at pH 7.4 at 37 °C. Texas Red® 1,2-dihexadecanoyl-*sn*-glycero-3-phosphoethanolamine, triethyl-ammonium salt (TR-DHPE) was from Invitrogen. All aqueous solutions were prepared with 18.3 MΩ.cm Milli-Q water. SMase buffer: 125 mM NaCl, 10 mM $CaCl_2$, 2 mM $MgCl_2$, 10 mM HEPES, pH 7.4.

2.2. Preparation of small unilamellar vesicles

Small unilamellar vesicles were prepared as previously described [24]. Briefly, chloroform solutions of phospholipids and fluorescently labeled lipids were mixed in the appropriate ratios and the lipid films obtained after drying the solvent were hydrated in water and vortexed to obtain multilamellar vesicles. The sample was then sonicated in a water bath sonicator (30–40 °C) to clarity to form small unilamellar vesicles with a final lipid concentration of 1 mM. Vesicles were used immediately for bilayer preparation or stored at 4 °C for up to a week prior to use.

2.3. Bilayer preparation

Vesicle solution (150 μl) and 300 μl $CaCl_2$ (15 mM) were added to freshly cleaved mica (60–70 μm thickness for fluorescence imaging) clamped in a liquid cell. After incubation at room temperature for 30 min bilayers were rinsed extensively with water to remove unattached vesicles before imaging. The presence of occasional defects allowed us to measure the bilayer thickness, confirming the presence of a single bilayer. Control experiments in which vesicle and bilayer preparation was carried out in a nitrogen atmosphere showed that bilayer morphologies for the ternary and quaternary lipid mixtures were similar for samples prepared under air and nitrogen. This indicates that lipid oxidation does not affect the results.

2.4. TIRF imaging

Fluorescence images of bilayers were taken on an Olympus 1X81 total internal reflection fluorescence (TIRF) microscope equipped with a high resolution CCD camera (CoolSNAP, Photometrics, US) and a 60x/1.45 NA Plan Apochromat objective. TR-DHPE was excited at 543 nm and emission collected at 593 (±20) nm.

For SMase treatment, the bilayers were washed with SMase buffer, and imaged. The effect of enzyme on the bilayer was followed in time by imaging the same area during and after addition of buffered enzyme solution at room temperature. SMase activity was assessed using an Amplex Red SMase assay kit from Molecular Probes.

2.5. AFM imaging

AFM images were obtained on a PicoSPM atomic force microscope (Molecular Imaging) in MAC-mode using magnetic coated silicon tips (MAClever Type II) with spring constants of ~0.5 N/m and resonance frequencies between 7 and 35 kHz in aqueous solutions. Either a 30×30 μm^2 or 5×5 μm^2 scanner was used with a scan rate between 0.7 and 1.3 Hz. All images shown are flattened raw data. Two or three independently prepared samples were imaged for each bilayer composition, and several areas were scanned for each sample. Domain heights were measured as the difference between the condensed phase domains and the fluid phase and 20 – 40 height estimates were collected per image. Results of several different experiments for each composition were used to generate histograms that were fitted with a Gaussian function. The reported heights are the peak of the Gaussian distribution.

For SMase treatment, the bilayers were imaged in water prior to replacing the water by buffered enzyme solution, incubated at room temperature for 2–30 min, rinsed extensively with water and re-imaged. None of the SMase-induced changes were observed in bilayers incubated with buffer alone, confirming that the membrane restructuring was not an artifact of the change in solution and electrolyte.

3. Results

3.1. Direct incorporation of ceramide in 5:5:1 DOPC/ESM/chol bilayers

Ternary lipid mixtures comprised of a saturated SM or PC, cholesterol and an unsaturated PC have been used to mimic the

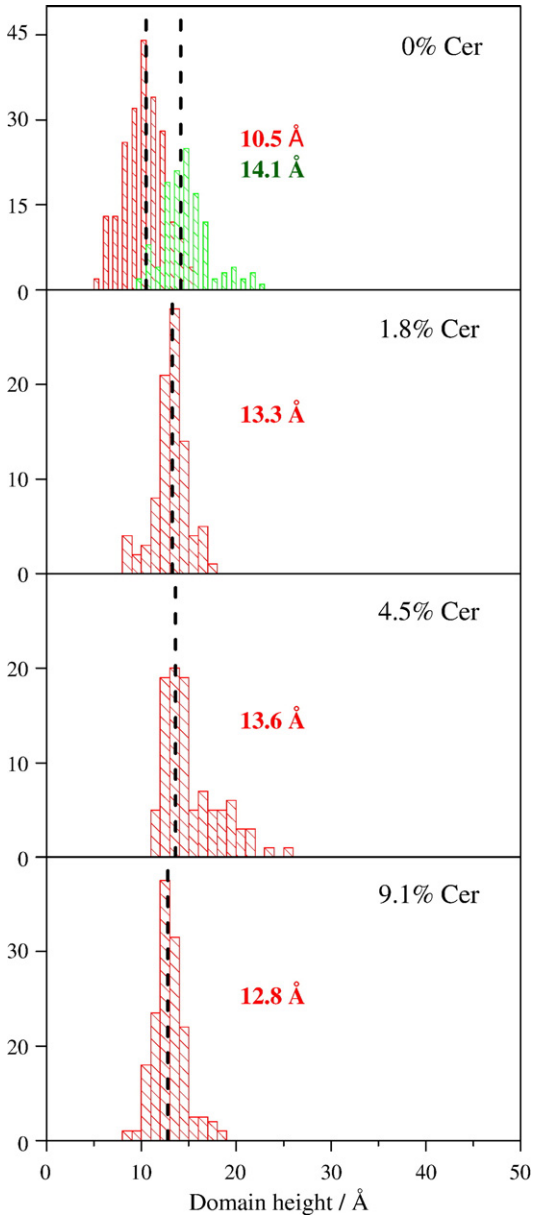

Fig. 2. Distribution of domain heights in ceramide containing bilayers. The histograms represent data from more than 2 independent experiments and the vertical black lines show peaks of the Gaussian fit with values indicated in Å. For 0% Cer the red and green columns are domain heights for 0–1 h and 1–3 h old bilayers, respectively. Domain heights decrease upon Cer addition. (For interpretation of the references to colour in this figure legend, the reader is referred to the web version of this article.)

behavior of lipid rafts in vesicles and supported membranes [1]. Our previous study of ceramide incorporation in supported lipid bilayers used a 2:2:1 DOPC/ESM/chol mixture (molar ratios, DEC 221) which exhibits phase separation to give ESM/chol rich liquid-ordered domains in a fluid DOPC-rich phase [24]. Similar mixtures show coexisting fluid phases in both giant vesicles and supported phospholipid bilayers [34–37]. In this work we used a lower mol fraction of cholesterol which has been shown to give small ordered nanodomains [34]. The AFM image in Fig. 1A shows a typical bilayer prepared from a 5:5:1 DOPC/ESM/chol mixture (DEC 551). The bilayer is heterogeneous with many small nanodomains ranging in size from tens of nanometers to a few hundred nanometers, randomly distributed in a fluid phase, in agreement with literature results [34]. The domain sizes are within the range of estimates for lipid rafts in cellular membranes [27].

The condensed phase domains were 10.5 Å high (Fig. 1A) and were irregular in shape with consequently large interfacial area. The DEC 551 bilayers were dynamic, with the domains increasing in size and height during the first 1–2 h after formation (Fig. 1B, size increased from a few tens of nm to a few hundreds of nm). Beyond 3 h the bilayers were stable when stored at room temperature in water for up to 24 h, with no further changes in either height or size of the domains. The height data is summarized in Fig. 2, 0% Cer. The domain heights in DEC 551 membranes show a broad distribution at both early (<1 h) and later (1–3 h) time points with the former showing a peak at 10.5 Å and the latter at 14.1 Å.

The major component of ESM being $C_{16:0}$ SM (85%), we chose $C_{16:0}$ ceramide for studying the effect of ceramide on the ordered nanodomains. Increasing amounts of ESM were replaced with $C_{16:0}$ ceramide in the DOPC/ESM/chol mixture such that the total mol% of ESM and ceramide remained constant at 45.5%. The total amount of ceramide was varied between 0 and 9% which is well within a physiologically relevant range [16,38]. The relatively low fraction of ceramide also avoids problems associated with obtaining reproducible bilayers by vesicle fusion for lipid mixtures with relatively large fractions of a high T_M lipid (T_M=90 °C for $C_{16:0}$Cer) [39,40].

Replacement of ESM with ceramide in the DEC 551 mixture resulted in significant changes in bilayer morphology. Fig. 1 shows the effect of increasing the membrane ceramide content from 0 to 9.1%. The condensed phase domains become progressively larger with increasing ceramide content, with some domains as large as approximately 1 μm in size for the 9.1% ceramide bilayer. At the same time the domains had smoother edges and consequently lower interfacial area, as compared to the small interconnected domains observed in the absence of ceramide. The distribution of domain heights (Fig. 2) showed a shift to lower heights with increasing ceramide content, varying from 14.1 Å for 0% Cer to 12.8 Å for 9.1% Cer, and did not change with time over a period of several hours. The surface area covered by domains increased slightly on addition of ceramide from 30±6% for 0% ceramide (an average of bilayers at various time points) to 36±4% for 9% ceramide.

3.2. In situ ceramide generation in DOPC/ESM/chol 551 with B. cereus SMase

In cellular rafts ceramide is generated by SMase catalyzed SM hydrolysis *in situ*. We have shown earlier that *in situ* ceramide generation in model rafts leads to significant membrane

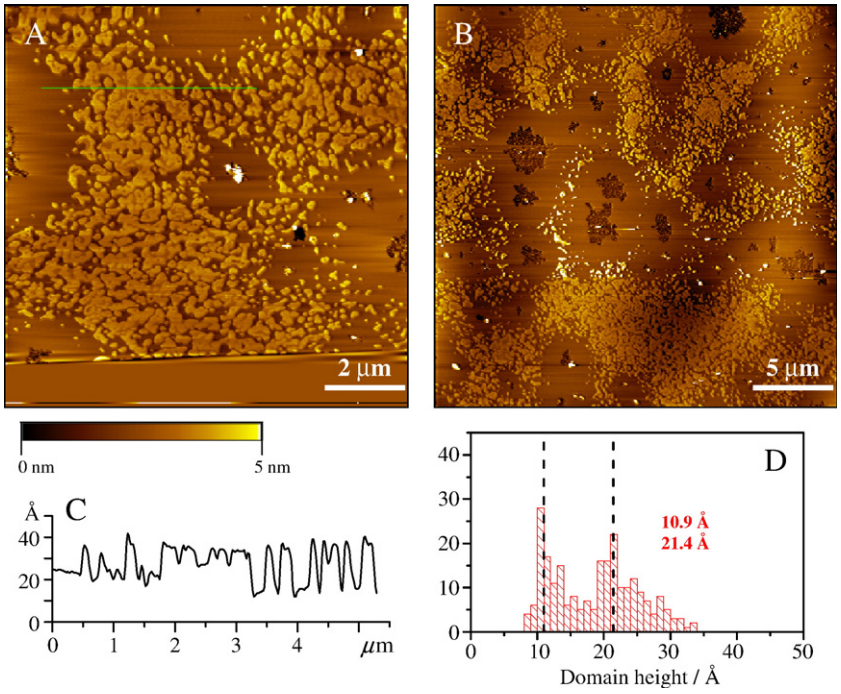

Fig. 3. DEC 551 bilayers treated with 0.1 U/ml SMase (*B. cereus*) for 15 min, washed with water and imaged (A) 8 min and (B) 16 min later. The domain size increased relative to a control bilayer (similar to Fig. 1B) and the domains clustered into large heterogeneous patches. (C) Cross section for the line indicated in image A shows that the domains have two distinct heights. The histogram of domain height distribution (D) is bimodal with peaks at 10.95 Å and 21.4 Å (vertical black lines).

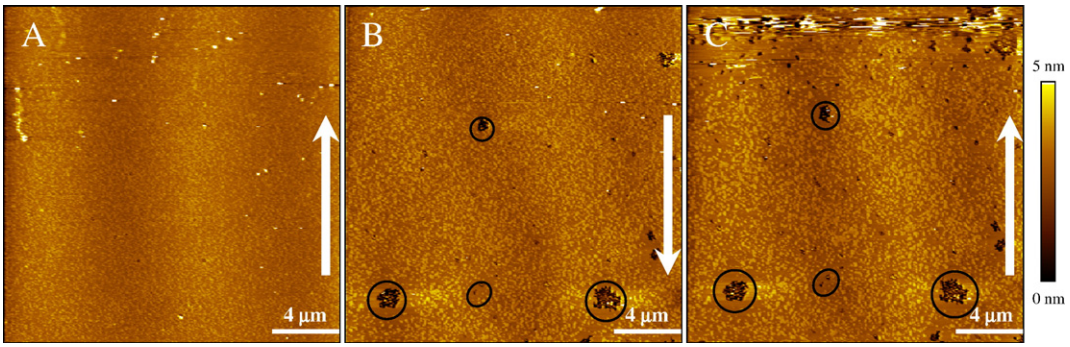

Fig. 4. DEC 551 bilayer before (A) and during (B, C) treatment with SMase (*B. cereus*). After imaging area (A), the buffer above the bilayer was replaced by flowing 1 ml of 0.05 U/ml SMase through the cell. The same area was then imaged (B) 1 min, and (C) 7 min later. The white arrows indicate the scan direction. The top part of image in panel C appears streaky due to tip contamination. The circles show areas of lower phase from which the domains have disappeared and many of which contain membrane defects.

restructuring which is not observed in bilayers prepared with premixed ceramide [24]. Therefore, it is important to study the effect of SMase-generated ceramide in raft bilayers for comparison with the effect of premixed ceramide in similar membranes.

DEC 551 bilayers were imaged after SMase treatment for comparison with the premixed ceramide/DEC mixtures described above. Freshly prepared bilayers were imaged first, then incubated with a buffered SMase solution for 2–15 min and washed extensively with water and re-imaged. Typical images for a DEC 551 bilayer after incubation with 0.1 U/ml of SMase for 15 min are shown in Fig. 3A, B. Comparison with images for the untreated bilayer shown in Fig. 1A, B indicates that SMase treatment leads to a strikingly restructured bilayer. Enzymatic generation of ceramide leads to several distinct features: (a) Individual domains are enlarged; whereas the domains in the untreated bilayer varied from tens to a few hundred nm in size (Fig. 1A, B), the SMase treated bilayers had domain sizes ranging from several hundred nm to a couple of µm (Fig. 3). (b) Large heterogeneous domain clusters could be distinguished in most areas. The heterogeneity is clearly visible in some of the clusters in Fig. 3A, C where an intermediate phase ~11 Å high is surrounded by a phase that is ~20 Å high (Fig. 3D). Some

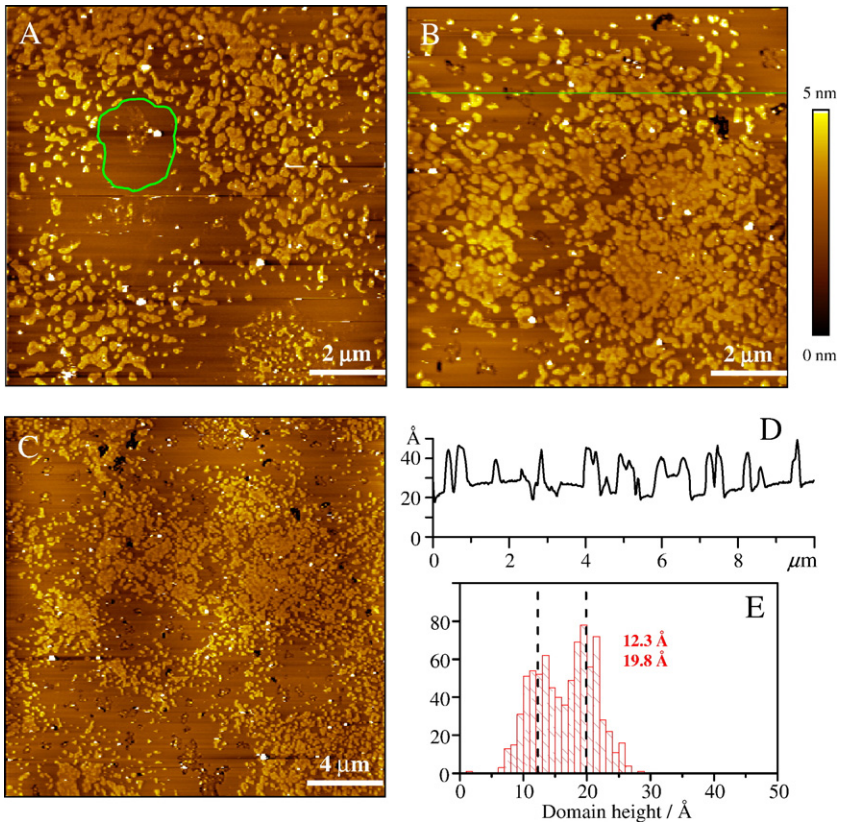

Fig. 5. DEC 551 bilayer treated with 1 U/ml SMase (*S. aureus*) for 15 min, washed with water and imaged (A) 29 min, and another area (B) 69 min and, (C) 76 min later. (D) Cross section for the line indicated in image B and (E) height distribution for domains in SMase treated bilayers. The domain size increased relative to the control and the domains clustered into large heterogeneous patches. Heterogeneous domains were 12.3 Å high with 19.8 Å high subdomains.

clustered domains retain small areas of the lower phase. (c) The SMase treated bilayer showed a non-random arrangement of domains with clusters of domains around the periphery of roughly circular areas of a lower phase that had occasional bilayer defects (Fig. 3B). This is in contrast to untreated bilayers which always showed a random distribution of nanodomains in the fluid phase. (d) The total area covered by the domains is slightly lower after enzyme treatment (26.6% for multiple images of the bilayer shown in Fig. 3).

It was possible to capture bilayer changes in the early stages of the enzyme reaction by imaging bilayers without washing out excess enzyme. In situ imaging was only carried out at low enzyme concentrations (<0.1 units/ml) due to problems associated with tip contamination at high SMase concentrations. The images in Fig. 4 show the evolution of the bilayer morphology in the early stages of SMase-induced bilayer changes after 1 ml of 0.05 U/ml was slowly flowed into the sample cell. Dilution of the enzyme solution by buffer in the AFM cell will give a final concentration of less than 0.05 U/ml SMase which is lower than the enzyme concentration used in Fig. 3. The effects of ceramide generation were evident even at the earliest time point imaged after enzyme injection (Fig. 4B). The domains were significantly enlarged compared to the control (Fig. 4A, note change in scale from Fig. 1). The circled areas in Fig. 4B and C mark regions of the bilayer where domains have been replaced by holes and/or a uniform lower phase. The bilayer in this case does not exhibit the same degree of membrane restructuring as in Fig. 3 presumably due to the lower SMase concentration. At longer time-scales (>1 h) the bilayer became progressively more unstable due to formation of large defects and ultimately only bilayer patches were observed (data not shown).

3.3. In situ ceramide generation in DOPC/ESM/chol 551 with S. aureus SMase

The results described in the previous section were obtained with a bacterial SMase purified from *B. cereus*. Since some batches of this enzyme may contain a minor phospholipase contaminant [41], we also used enzyme from a different bacterial source, *S. aureus*, to confirm that our observations of SMase-induced changes in 551 bilayers are due only to ceramide generation. Both bacterial SMases have been used extensively to study the effect of ceramide on model membranes, although to the best of our knowledge this study and our previous work [24] are the only studies that report a direct comparison of the two enzymes.

DEC 551 bilayers were treated with SMase as outlined above and imaged after washing. Typical images for a DEC 551 bilayer after treatment with 1 U/ml SMase are shown in Fig. 5A–C. The results parallel those obtained when ceramide is generated with *B. cereus* SMase. Individual domains were larger, ranging in size from several hundred nm to a couple of μm (Fig. 5A, B) and large heterogeneous domain clusters exhibiting phases with

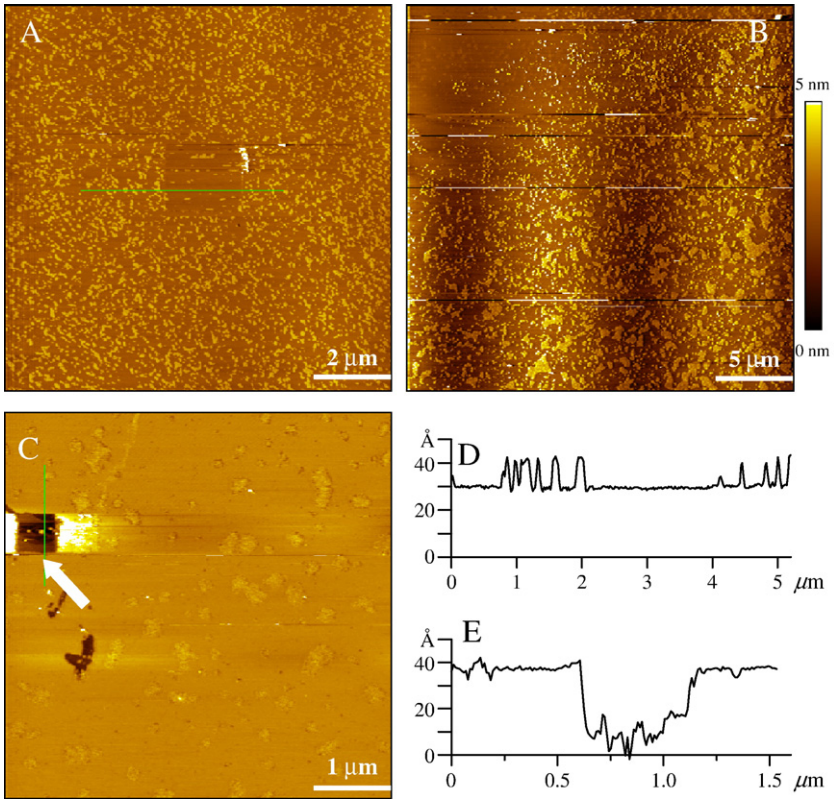

Fig. 6. (A) DEC 551 bilayer imaged after scanning a 2×2 μm^2 area at high force in contact-mode; cross section (D) for the line indicated in image A shows fluid phase with few remaining domains rather than a bilayer defect. (B and C) SMase treated 551 bilayer (same experimental conditions as in Fig. 5). The upper left part of image (B) shows an area of lower phase in which a 0.5×0.5 μm^2 region was scanned at high force in contact mode. Re-imaging this area (C) clearly shows the hole generated; the cross section (E) for the line across the hole in image C indicates a bilayer thickness of ~40 Å.

average thickness of 12.3 Å and 19.8 Å were observed. The bilayer also showed a non-random arrangement of domains clustered around the periphery of large irregularly shaped areas of a lower phase with relatively few bilayer defects (Fig. 5A, C). Some areas of lower phase had clustered domains in the centre (circled area in Fig. 5A). The total area covered by the domains is slightly higher after enzyme treatment (34.5±6.5% for multiple images of the bilayers shown in Figs. 5 and 6). This is in contrast to results obtained with *B. cereus* SMase which showed an apparent decrease in domain surface coverage; however, the more frequent defects obtained for this enzyme may contribute to the apparent decrease in the surface area covered by the domains.

The above noted bilayer changes for *S. aureus* SMase were observed only at high enzyme concentrations (≥1 U/ml). At lower concentration (0.1 U/ml, Supplementary material) SMase induced less clustering and membrane reorganization, and more defects — both large and small. Comparison of the ceramide yield for the two enzymes for detergent solubilized sphingomyelin showed a slightly higher activity for *B cereus*, but by less than a factor of 2. However, the relative activities of the two enzymes may be different with respect to a supported bilayer.

To examine the fluidity of the large areas of lower phase that are observed after enzyme treatment, we attempted to scratch a hole by scanning a small area (500 nm × 500 nm) at high force in contact mode. The results of this experiment for bilayers before and after treatment with enzyme are illustrated in Fig. 6. Fig. 6A for an untreated bilayer shows a small square of lower phase with very few domains in the centre of the image, indicating that lipids displaced by the probe are rapidly replaced by lipids in the liquid-disordered phase (DOPC). Fig. 6B shows a SMase-treated bilayer with a large patch of lower phase in its upper left hand corner; the same area is imaged again after scanning at high force and shows a large hole (~4 nm deep, Fig. 6C, E) in the bilayer. This indicates that the lower phase is less fluid than the original DOPC-rich phase prior to enzyme treatment, consistent with formation of a more ordered phase by redistribution of lipids in response to ceramide generation. Ceramide-induced bilayer restructuring may involve displacement of cholesterol into the DOPC-rich phase to give a liquid-ordered phase in which holes in the bilayer are stable on the AFM timescale. Such stable holes however, could not be produced in all areas, suggesting heterogeneity in this phase as well. This presumably

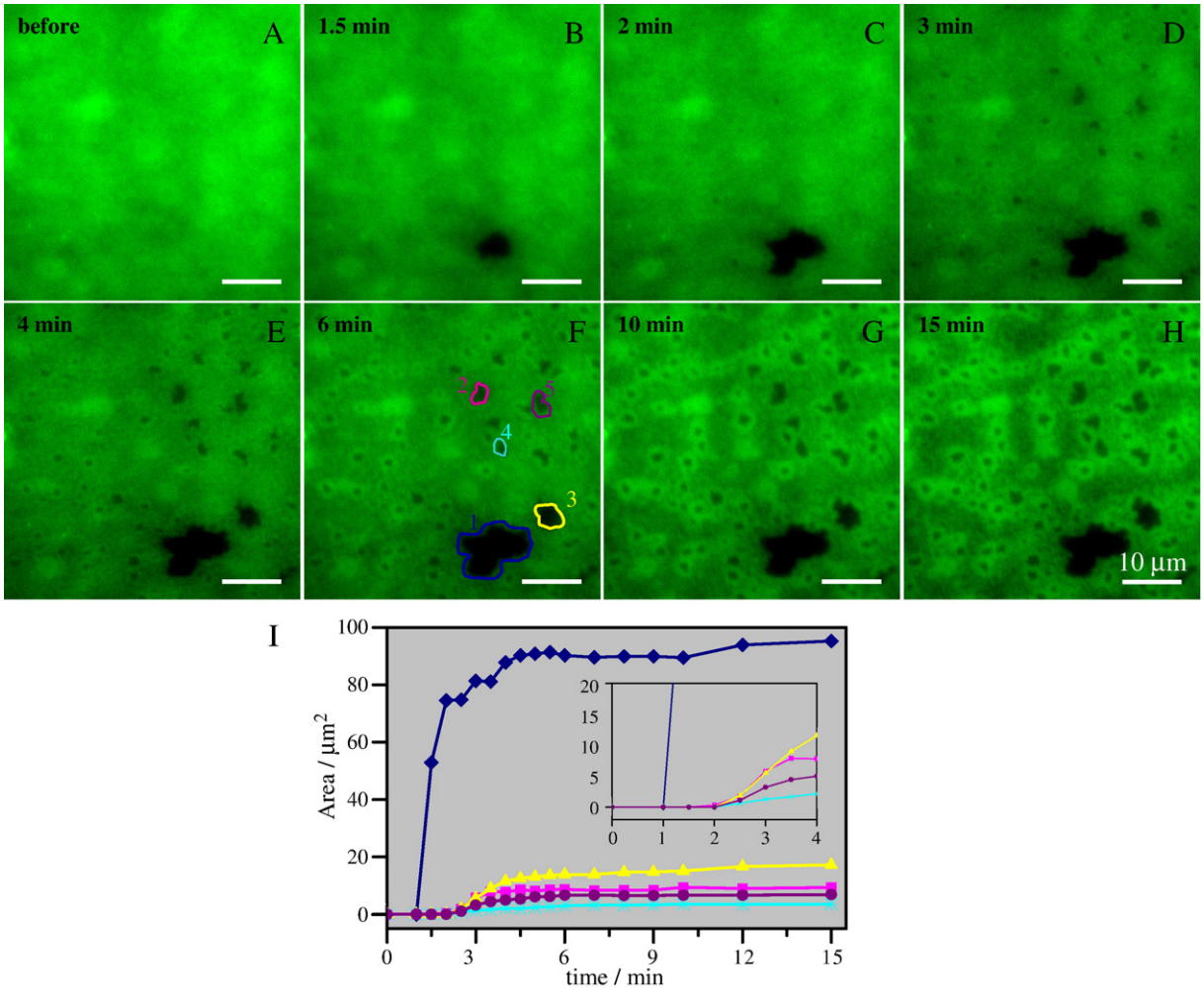

Fig. 7. Following SMase (*S. aureus*) mediated bilayer changes in real time with TIRF microscopy. A DEC 551 bilayer with 0.5% TR-DHPE was imaged before (A) and at various times after (B–H) injection of 1 U/ml SMase. (I) Areas of "domains" 1–5 (outlined in panel F) were plotted as a function of time after enzyme injection; the inset shows initial slopes of the curves. The graphs show that the dark patches expand rapidly during the first 0–4 min and then reach a plateau at later times.

reflects the low overall fraction of cholesterol in the bilayer and the heterogeneity in the enzymatic generation of ceramide.

3.4. Following the time-course of SMase-induced membrane changes with TIRF microscopy

Fluorescence experiments were employed to provide a more detailed picture of the time evolution of the ceramide-induced bilayer restructuring. DEC 551 bilayers were prepared with 0.5% TR-DHPE and imaged in TIRF mode. The headgroup labeled fluorescent lipid is known to partition into the fluid-phase giving rise to "dark" domains in fluorescence images [42]. The TIRF image for an untreated DEC 551 bilayer in Fig. 7A shows uniform fluorescence throughout the bilayer. As expected, the small, closely spaced domains observed by AFM are not resolvable with the diffraction limited resolution of the TIRF microscope.

The time course of enzyme-induced changes in the bilayer was followed by imaging the bilayer at regular intervals after injection of enzyme (*S. aureus*). Fig. 7 shows a typical series of fluorescence images obtained for a bilayer to which 1 U/ml SMase was added. Selected time-points are shown in Fig. 7B–H. Changes in the bilayer are evident as early as 1.5 min after SMase addition — a small dark patch forms at the lower right corner of the image and appears enlarged in the next image. In 3 min (Fig. 7D) several more of these dark patches can be observed and they expand rapidly in the next 2–3 min. At 4 min bright circular areas around some of the dark patches are observed and they are well developed by 6 min (Fig. 7F). At the end of 15 min (Fig. 7H) the SMase-treated bilayer exhibits the following main features: (i) micron-sized dark patches, (ii) bright circular areas around some of the dark patches, and (iii) areas of intermediate fluorescence. The sizes and numbers of the various features vary considerably throughout the sample, presumably reflecting the random nature of the initial enzyme interaction with the bilayer.

A quantitative analysis of the rate of expansion of the dark patches was performed over a time interval of 15 min after enzyme injection. Fig. 7I shows the result of a typical kinetic analysis for the features outlined in Fig. 7F where the area of individual patches has been plotted as a function of time after SMase addition. The patches expand rapidly in the first 0–4 min after their appearance and level off thereafter. Most of these expanding patches are between 1 and 5 μm in size (areas 2–5 in Fig. 7F) but a significant number (1–2 in each 50 μm image) of much larger dark patches (7–15 μm, feature 1 in Fig. 7F) were also observed in each area imaged. Individual patches expand at different rates as can be seen from the initial slopes shown as an inset in Fig. 7I. This suggests that each dark patch reflects the activity of a different number of enzyme molecules. Further, there is a lag time between enzyme injection and the appearance of dark areas that is different for each patch.

For comparison with the AFM experiments, the bilayer imaged in Fig. 7 was washed extensively with water ~16 min after enzyme addition and then reimaged. Fig. 8A, B show images recorded immediately and 50 min after washing. Over this time period the dark patches continued to enlarge and the

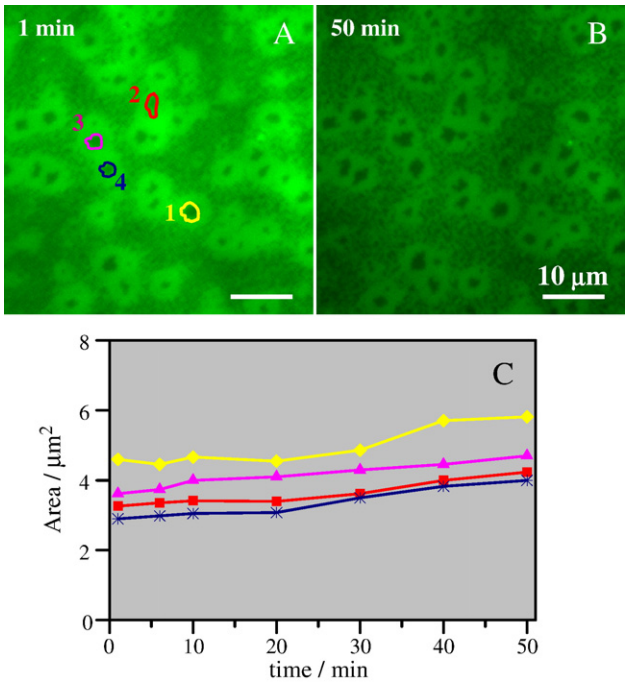

Fig. 8. The bilayer in Fig. 7 was washed 15 min after enzyme injection and a different area was imaged 1 (A) and 50 min (B) after washing. The graph in (C) shows slow expansion of "domains" 1–4 outlined in (A).

areas of intermediate fluorescence became more clearly resolved as dark micron-sized interconnected domains interspersed with a fluorescent phase. The slow increase in domain size over time is illustrated in Fig. 8C where the area of the features numbered in Fig. 8A was plotted as a function of time after washing off the enzyme. The slow change in the bilayer after removal of the enzyme is attributed to continued redistribution of lipids in response to ceramide generation.

Comparison of the TIRF and AFM data suggests that the dark patches with surrounding bright rings of fluorescence observed via TIRF correspond to the clustered domains detected by AFM. For example, the feature highlighted in Fig. 5A shows a small cluster of domains enclosed in a circular area of a uniform fluid phase. Ceramide generation and concomitant cholesterol expulsion into the surrounding DOPC and TR-rich phase will lead to dye expulsion from the domain cluster giving rise to the large "dark" domains. An alternate possibility is that some of the dark patches correspond to defects, but we think this is unlikely for *S. aureus* SMase for which relatively few and quite small defects are observed in AFM images (see Fig. 5). The occasional considerably larger dark patches in TIRF images may correspond to large areas of clustered domains, as for example in the area marked in Fig. 5A. The frequent large areas of intermediate fluorescence intensity in the TIRF images are assigned to regions where there are enlarged and clustered domains that retain significant levels of fluid phase and entrapped dye.

4. Discussion

Ceramide incorporation leads to enlargement of nanoscale ordered domains in DEC 551 bilayers, irrespective of its mode of addition. Enzymatic ceramide generation also leads to a

large-scale membrane reorganization that can be detected in the first few minutes of enzyme activity and involves changes in distribution and aggregation of domains in the membrane, as well as increased heterogeneity of individual domains. Overall, the results highlight the diverse effects of ceramide in ternary lipid mixtures and provide data of relevance to the frequently postulated coalescence of raft domains in cellular membranes.

4.1. Direct ceramide incorporation modifies domain morphology

The DEC 551 mixture formed heterogeneous bilayers with small domains that increased in height and size during the first 1–2 h after formation. The final stable bilayer had domains that were ~14 Å higher than the fluid phase, slightly larger than the ~11 Å height difference measured previously for domains in DEC 221 bilayers [24]. The variations in domain thickness and size as a function of cholesterol content are consistent with a previous AFM study of DOPC/SM/chol bilayers [43]. X-ray diffraction studies for SM/chol bilayers have also found that cholesterol reduces the membrane thickness, presumably by disrupting the packing of SM lipid chains [44]. No changes in domain morphology with time were observed in our previous study of DEC 221 bilayers. However, bilayers prepared from several phase separated binary lipid mixtures have been shown to undergo considerable equilibration of domain size, thickness and coupling, depending on their thermal history [45–47]. Moreover, a recent study by Longo and coworkers has demonstrated that the addition of cholesterol decreases the time required to obtain an equilibrium domain morphology [47]. Based on this observation, one would predict that the relatively low cholesterol content (9%) in DEC 551 bilayers would increase the time required to achieve an equilibrium bilayer morphology. The changes observed during the first 2 h after bilayer preparation are thus attributable to membrane domain equilibration. The domain enlargement is accompanied by a slight height increase that may reflect more tightly packed domains. The smaller domains are more likely to be compressed by the AFM tip, which may also contribute to a lower apparent height. We see no evidence for domain asymmetry, indicating that domains are coupled through both leaflets as is typical in ternary lipid mixtures.

Direct ceramide incorporation in the vesicles used to prepare supported bilayers leads to significant changes in the bilayer morphology. The domains are substantially larger with more uniform, rounded shapes, the height difference between the domains and surrounding fluid phase decreases and the surface area covered by the domains increases slightly. It is interesting to note that these effects are qualitatively similar to those observed when increasing amounts of cholesterol are added to SM/DOPC mixtures [34], although it takes considerably less ceramide than cholesterol to achieve a comparable change in domain morphology. The increased surface area covered by domains after ceramide incorporation suggests that SM is recruited from the fluid phase; the recruitment of SM more than compensates for the condensing effect expected upon replacement of SM with ceramide or for any loss of cholesterol from the domains [16].

The similarity between the effects of adding ceramide and cholesterol has been noted in two other recent studies. First, a detailed investigation by Prieto demonstrated that ceramide strongly modifies the membrane properties of POPC/SM/chol vesicles at low cholesterol mol fraction; remarkably, 2% ceramide had a similar ordering effect to 25% cholesterol in POPC/SM mixtures [26]. This work also concluded that ceramide recruits SM from the liquid-disordered to the gel phase [26] with one ceramide being capable of recruiting 2–3 SM molecules. A second study has concluded that asymmetric ceramides may act in a similar way to cholesterol, making gel phases more fluid and fluid phases more gel-like [48].

The effects of ceramide addition to DEC 551 bilayers differ in two respects from earlier observations for DOPC/SM/chol mixtures with a larger cholesterol mol fraction (20 and 33% [17,24]). First, samples with 2–9% ceramide provide no evidence for the ceramide-enriched islands that are formed within the ordered domains when 10% ceramide is added to DEC 221 bilayers [24]. We hypothesize that this is due to the higher SM/ceramide ratio in the present study (5:1 for 9% ceramide vs. 3:1 for 10% in DEC 221). Second, neither of the previous AFM studies of ceramide addition to SM/chol/DOPC mixtures with large (micron-sized) domains reported enlargement of individual domains. Similarly Prieto found no evidence for changes in raft size when ceramide was added to POPC/SM/chol mixtures, at least at low ceramide concentrations [26]. We attribute the significant effects of ceramide on domain size for DEC 551 bilayers to the lower mol fraction of cholesterol which gives gel phase rather than liquid-ordered domains [49]. Thus, it is clear that the behavior of ceramide is complex and varies significantly with lipid composition.

4.2. SMase promotes enlargement and clustering of nanodomains

Enzymatic generation of ceramide leads to a remarkable restructuring of DEC 551 bilayers that is quite distinct from the effects of direct ceramide incorporation, in agreement with previous results for DEC 221 bilayers. The restructured bilayer shows two distinct features by AFM, clusters of larger heterogeneous domains with two distinct phases and adjacent areas of a uniform lower phase that is devoid of domains. A detailed comparison of AFM, fluorescence and effects of enzyme concentration and exposure time allow us to draw several conclusions concerning this membrane reorganization.

Enzymatic generation of ceramide consistently yields an increase in the size of individual domains that occurs rapidly on the AFM timescale. Individual domains have two distinct heights (11–12 and ~20 Å above the surrounding lower phase), and are usually clustered together with occasional small areas of entrapped lower phase. The highest phase of the clustered domains can reasonably be assigned to a new ceramide-rich phase. Several studies have reported the direct AFM visualization of three coexisting phases when ceramide is generated enzymatically in bilayers of ternary lipid mixtures. [17,24,25]; similarly, three coexisting phases have been observed when ceramide is premixed with ternary lipid mixtures [17,24,26]. These findings corroborate earlier work that documented phase separation to

give ceramide-rich domains or platforms in lipid monolayers and vesicles with fewer lipid components [20,21,23,50–54].

Our earlier study of enzymatic ceramide generation in DEC 221 membranes demonstrated that the new ceramide-rich phase was localized at the edges of the model raft domains [17,24], consistent with enzyme activity at the interface between the liquid-ordered and liquid-disordered phases. The new higher phase is present in larger amount and is more heterogeneously distributed in DEC 551 bilayers. We attribute this to the fact that the large perimeter of the small initial domains facilitates conversion of a greater fraction of the SM to ceramide. Consistent with this, we find that >60% of the initial SM is hydrolysed upon *B cereus* SMase treatment of DEC 551 bilayers, compared to 20–40% SM hydrolysis in DEC 221 bilayers under similar conditions [24]. The high local concentration of ceramide will contribute to the differences observed upon enzymatic treatment of bilayers with varying amounts of cholesterol as well as to the difference between direct and enzymatic ceramide incorporation. When ceramide is premixed in vesicles used to prepare supported bilayers, there is ample time to achieve an equilibrium distribution of components, yielding a more homogeneous membrane. By contrast, in enzyme-treated bilayers ceramide is heterogeneously distributed laterally within the domains and is also asymmetrically distributed between the two leaflets of the same domain. Ceramide flip-flop between leaflets as well as lateral redistribution of lipids may both contribute to the changes in bilayer morphology that occur over timescales from minutes to hours following enzyme generation of ceramide.

The islands of a new higher phase produced by ceramide incorporation have been assigned to a ceramide-enriched gel phase that probably also contains SM in two previous studies [17,24]. Although this is consistent with trends in both direct and enzymatic incorporation of ceramide, the height difference is larger than predicted for either a SM or ceramide gel phase. We propose that the surface asymmetry created by replacing SM with a lipid having a smaller head group promotes ceramide flip-flop to the lower leaflet and that the higher regions of the bilayer are due to ceramide-enriched regions in the lower leaflet that are slightly raised from the surface by virtue of the negative membrane curvature induced by ceramide. The cartoon in Fig. 9 illustrates this hypothesis. A number of studies have documented ceramide flip-flop between membrane leaflets in vesicles and cell membranes [7,11,13,14]; estimates for the half-life for ceramide flip-flop range from 22 min to less than 1 min at 37 C [13,55]. It has been suggested that rapid flip-flop is caused by a combination of the transient formation of non-lamellar structures and the tendency to minimize lateral tension in each membrane leaflet [7]. In the case of supported bilayers, rapid lipid exchange between leaflets may also be facilitated by the formation of short-lived bilayer defects induced by enzyme activity, consistent with defects observed by AFM in this work and related studies [24,25]. The small elevated features observed by AFM for Langmuir–Blodgett bilayers with anionic lipid initially only in the upper leaflet have similarly been attributed to lipid exchange at defect sites, coupled with electrostatic repulsion between anionic lipids in the lower leaflet and the mica surface [56]. Reversible formation of three-dimensional raised structures by modulation of ionic strength for bilayers containing phosphatidic acid has also been reported recently [57]. Moreover, ceramide flip-flop and negative membrane curvature have been postulated to explain the effects of SMase on vesicle membranes [20,25]. This further supports our hypothesis that the negative curvature of ceramide leads to anomalously high ceramide rich domains observed in SMase treated bilayers.

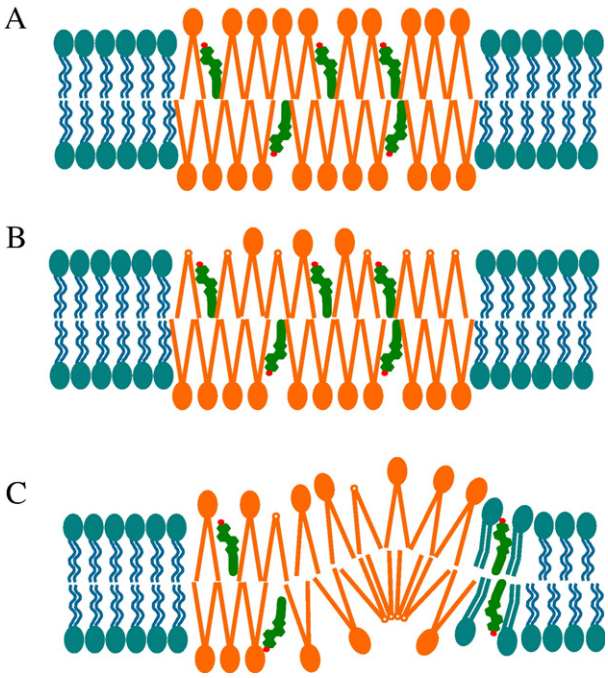

Fig. 9. Model to explain the formation of higher domains upon enzymatic generation of ceramide. The initial bilayer (A) has coexisting disordered (DOPC-rich) and ordered (SM and chol-rich) phases. (B) Ceramide generated by enzymatic hydrolysis of SM in the upper leaflet results in bilayer asymmetry. This leads to lipid exchange between leaflets and to displacement of cholesterol from the ordered domains (C). Ceramide in the lower leaflet leads to a negative membrane curvature that produces the higher subdomains observed by AFM.

Our data provide strong evidence that the large areas of lower phase produced by enzyme treatment are more ordered than the original DOPC-rich liquid-disordered phase. This is illustrated by the fact that stable bilayer defects can be created in some areas of the lower phase after SMase exposure, whereas the lower fluid phase is too mobile to maintain defects in untreated DEC 551 bilayers. Expulsion of cholesterol from the domains into the lower DOPC-rich phase for SMase treated membranes [16] may explain the increased order for some areas of the lower phase. Not all areas of the lower phase were sufficiently ordered to allow formation of a stable bilayer hole, suggesting considerable heterogeneity in the distribution of cholesterol within the fluid phase and consistent with the relatively low mol fraction of cholesterol in DEC 551 bilayers.

Comparison of TIRF and AFM images indicates that the large domain clusters observed by AFM appear as dark patches in fluorescence mode. Some of these are encircled by brightly fluorescent rings of a fluid phase that incorporates dye. Other areas of the TIRF images have an intermediate fluorescence

intensity that is attributed to a combination of individual domains with small regions of entrapped fluid phase. Based on the combined AFM and TIRF data, we hypothesize that the large clusters of domains form at sites of relatively high enzyme activity. Small individual domains enlarge and become heterogeneous with ceramide-rich and SM-rich regions and some cholesterol may be displaced to the surrounding fluid phase. Coalescence or clustering of domains with concomitant redistribution of fluid phase to the periphery of the domain clusters occurs relatively rapidly over a timescale of a few minutes, although there is a slower membrane evolution that continues over a longer time period. The amount of membrane restructuring is less when the enzyme concentration is reduced by ten-fold. However, the bilayer morphology is even more heterogeneous from area to area and sample to sample, making it difficult to draw quantitative conclusions.

AFM images at low enzyme concentration show that the first detectable changes occur rapidly, within approximately 1 min after enzyme addition. Fluorescence imaging allows one to monitor the time evolution of the bilayer over a wider range of timescales, although at substantially lower spatial resolution. The large dark patches assigned to clustered domains grow in during the first 5 min of enzyme exposure. This is followed by a slower change in the next 60–80 min that does not require enzyme activity. The large dark patches vary in size and grow at different rates, consistent with activity of different numbers of enzymes in individual areas of the membrane. This explains the considerable variability observed between different areas of the enzyme treated bilayers (see for example Figs. 2–5). A combination of surface pressure changes and the growth of dark ceramide-rich domains that exclude dye has been employed for a detailed kinetic analysis of SMase activity in SM monolayers [51,58]. The authors conclude that diffusion-limited partitioning of SMase to the interface is followed by a lag time due to slow enzyme activation at the monolayer surface, during which the number of dark domains increases. This is followed by a phase in which SM to ceramide conversion occurs rapidly with individual domains increasing in size in an approximately linear manner and the kinetics reaching a transient steady state rate. The rate of SM hydrolysis then levels off as ceramide enrichment limits substrate availability. The kinetic data from the TIRF experiments fit this model reasonably well, with the added feature of a continued slow evolution of the bilayer following enzyme inactivation.

4.3. Summary and biological implications

We have shown that ceramide addition promotes significant changes in domain morphology and membrane organization for supported bilayers with small nanometer-sized ordered domains. There are significant differences between direct incorporation and enzymatic generation of ceramide, with the latter having a more pronounced impact on membrane organization. Undoubtedly, the most striking observation is the enlargement and clustering or coalescence of individual nanodomains following enzyme treatment of the bilayer. A number of studies have hypothesized that ceramide can promote the formation of large signaling platforms, and a few have provided direct evidence for large ceramide-rich domains [8,10]. However, to the best of our knowledge, the results described here provide the first direct visualization of ceramide-induced coalescence or clustering of small nanometer-sized domains to give large ordered domains. Although it is tempting to equate this to the postulated conversion of small rafts to large signaling platforms, several caveats should be kept in mind. First, the small nanosized domains for the DEC 551 mixture are still in the solid phase due to the relatively low cholesterol concentration. Second, the amount of ceramide generated is relatively high; although enzyme activity at membrane surfaces will generate a high local concentration of ceramide, the present system may still be far from physiological conditions. Despite these limitations, it is particularly interesting to note the variation in membrane restructuring exhibited by the two DOPC/SM/chol mixtures that we have examined. Thus, in more complex cellular membranes ceramide generation is anticipated to have diverse consequences that are extremely sensitive to the level of enzyme activity and initial lipid composition.

As noted above, the direct incorporation of ceramide gives different results to those induced by SMase, although enlargement of individual domains is still observed. Interestingly, the changes in domain morphology are analogous to those induced by chol, highlighting the fact that ceramide can modulate lipid ordering and/or induce gel phase domain formation, depending on membrane composition. While differences between direct and enzymatic ceramide incorporation have been documented in several studies [51,52,59], we have now demonstrated that these conclusions apply to more complex lipid mixtures that better model cell membranes. Despite the valuable biophysical data available from mixtures with an equilibrium distribution of lipids, it is crucial to consider the added complexity derived from the generation of high local concentrations of ceramide by enzyme activity.

Finally, the present work plus recent studies of phase diagrams for ceramide containing mixtures [23,26] clearly illustrate the complexity of effects of ceramide on ternary lipid mixtures that are used to model membrane rafts. It would be advantageous to correlate AFM and fluorescence imaging of the effects of enzyme treatment for membranes where the initial ordered domains are in a liquid-ordered phase but are nanometer in size. Based on the limited data available for two lipid mixtures, we anticipate a pronounced dependence of membrane reorganization on the size of the initial domains and their cholesterol content, as recently concluded by Prieto for a similar ternary lipid mixture using different techniques [26]. Combining the nanoscale spatial resolution of AFM with fluorescence imaging will be especially useful in understanding the diverse effects of ceramide in supported bilayers.

Appendix A. Supplementary data

Supplementary data associated with this article can be found, in the online version, at doi:10.1016/j.bbamem.2007.09.021.

References

[1] K. Simons, W.L. Vaz, Model systems, lipid rafts and cell membranes, Annu. Rev. Biophys. Biomol. Struct. 33 (2004) 269–295.

[2] K. Simons, E. Ikonen, Functional rafts in cell membranes, Nature 387 (1997) 569–572.

[3] A. Laude, I.A. Prior, Plasma membrane microdomains: organization, function and trafficking, Mol. Membr. Biol. 21 (2004) 193–205.

[4] D.A. Brown, E. London, Functions of lipid rafts in biological membranes, Annu. Rev. Cell Dev. Biol. 14 (1998) 111–136.

[5] M. Edidin, The state of lipid rafts: from model membranes to cells, Annu. Rev. Biophys. Biomol. Struct. 32 (2003) 257–283.

[6] A.E. Cremesti, F.M. Goni, R. Kolesnick, Role of sphingomyelinase and ceramide in modulating rafts: do biophysical propoerties determine biologic outcome? FEBS Lett. 531 (2002) 47–53.

[7] F.M. Goni, A. Alonso, Biophysics of sphingolipids I. Membrane properties of sphingosine, ceramides and other simple sphingolipids, Biochim. Biophys. Acta 1758 (2006) 1902–1921.

[8] C.R. Bollinger, V. Teichgraber, E. Gulbins, Ceramide-enriched membrane domains, Biochim. Biophys. Acta 1746 (2005) 284–294.

[9] F.M. Goni, A. Alonso, Sphingomyelinases: enzymology and membrane activity, FEBS Lett. 531 (2002) 38–46.

[10] H. Grassme, V. Jendrossek, A. Riehle, G. von Kurthy, J. Berger, H. Schwarz, M. Weller, R. Kolesnick, E. Gulbins, Host defense against *Pseudomonas aeruginosa* requires ceramide-rich membrane rafts, Nat. Med. 9 (2003) 322–330.

[11] F.X. Contreras, A.V. Villar, A. Alonso, R.N. Kolesnick, F.M. Goni, Sphingomyelinase activity causes transbilayer lipid translocation in model and cell membranes, J. Biol. Chem. 278 (2003) 37169–37174.

[12] R.N. Kolesnick, F.M. Goni, A. Alonso, Compartmentalization of ceramide signaling: physical foundations and biological effects, J. Cell. Physiol. 184 (2000) 285–300.

[13] I. Lopez-Montero, N. Rodriguez, S. Cribier, A. Pohl, M. Velez, P.F. Devaux, Rapid transbilayer movement of ceramides in phospholipid vesicles and in human erythrocytes, J. Biol. Chem. 280 (2005) 25811–25819.

[14] F.X. Contreras, G. Basanez, A. Alonso, A. Herrmann, F.M. Goni, Asymmetric addition of ceramides but not dihydroceramides promotes transbilayer (flip-flop) lipid motion in membranes, Biophys. J. 88 (2005) 348–359.

[15] Megha, O. Bakht, E. London, Cholesterol precursors stabilize ordinary and ceramide-rich ordered lipid domains (lipid rafts) to different degrees, J. Biol. Chem. 281 (2006) 21903–21913.

[16] Megha, E. London, Ceramide selectively displaces cholesterol from ordered lipid domains (rafts): implications for lipid raft structure and function, J. Biol. Chem. 279 (2004) 9997–10004.

[17] S. Chiantia, N. Kahya, H. Ries, P. Schwille, Effects of ceramide on liquid-ordered domains investigated by simultaneous AFM and FCS, Biophys. J. 90 (2006) 4500–4508.

[18] M.R. Ali, K.H. Cheng, J. Huang, Ceramide drives cholesterol out of the ordered lipid bilayer phase into the crystal phase in 1-palmitoyl-2-oleoyl-sn-glycero-3-phosphocholine/cholesterol/ceramide ternary mixtures, Biochemistry 45 (2006) 12629–12638.

[19] C. Yu, M. Alterman, R.T. Dobrowsky, Ceramide displaces cholesterol from lipid rafts and decreases the association of the cholesterol binding protein caveolin-1, J. Lipid Res. 46 (2005) 1678–1691.

[20] J.M. Holopainen, M.I. Angelova, P.K.J. Kinnunen, Vectorial budding of vesicles by asymmetrical enzymatic formation of ceramide in giant liposomes, Biophys. J. 78 (2000) 830–838.

[21] T.A. Nurminen, J.M. Holopainen, H. Zhao, P.K. Kinnunen, Observation of topical catalysis by sphingomyelinase coupled to microspheres, J. Am. Chem. Soc. 124 (2002) 12129–12134.

[22] Y. Taniguchi, T. Ohba, H. Miyata, K. Ohki, Rapid phase change of lipid microdomains in giant vesicles induced by conversion of sphingomyelin to ceramide, Biochim. Biophys. Acta 1758 (2006) 145–153.

[23] L. Silva, R.F.M. de Almeida, A. Federov, A.P.A. Matos, M. Prieto, Ceramide-platform formation and induced biophysical changes in a fluid phospholipid membrane, Mol. Membr. Biol. 23 (2006) 137–148.

[24] Ira, L.J. Johnston, Ceramide promotes restructuring of model raft membranes, Langmuir 22 (2006) 11284–11289.

[25] I. Lopez-Mentero, M. Velez, P.F. Devaux, Surface tension induced by sphingomyelin to ceramide conversion in lipid membranes, Biochim. Biophys. Acta 1768 (2007) 553–561.

[26] L.C. Silva, R.F.M. de Almeida, B.M. Castro, A. Fedorov, M. Prieto, Ceramide-domain formation and collapse in lipid rafts: Membrane reorganization by an apoptotic lipid, Biophys. J. 92 (2007) 502–516.

[27] L.J. Pike, Rafts defined: a report on the Keystone symposium on lipid rafts and cell function, J. Lipid Res. 47 (2006) 1597–1598.

[28] S.D. Connell, A. Smith, The atomic force microscope as a tool for studying phase separation in lipid membranes, Mol. Membr. Biol. 23 (2006) 17–28.

[29] Y.F. Dufrene, G.U. Lee, Advances in the characterization of supported lipid films with the atomic force microscope, Biochim. Biophys. Acta 1509 (2000) 14–41.

[30] P.E. Milhiet, M.-C. Giocondi, C. Le Grimellec, AFM imaging of lipid domains, TheScientificWorldJOURNAL 3 (2003) 59–74.

[31] L.J. Johnston, Nanoscale imaging of domains in supported lipid membranes, Langmuir 23 (2007) 5886–5895.

[32] C. Yuan, J. Furlong, P. Burgos, L.J. Johnston, The size of lipid rafts: an atomic force microscopy study of ganglioside GM1 domains in sphingomyelin/DOPC/cholesterol membranes, Biophys. J. 82 (2002) 2526–2535.

[33] J.E. Shaw, J. Oreopoulos, D. Wong, J.C.Y. Hsu, C.M. Yip, Coupling evanescent-wave fluorescence imaging and spectroscopy with scanning probe microscopy: challenges and insights from TIRF-AFM, Surf. Interface Anal. 38 (2006) 1459–1471.

[34] H.A. Rinia, M.M.E. Snel, J.P.J.M. van der Eerden, B. de Kruijff, Visualizing detergent resistant domains in model membranes with atomic force microscopy, FEBS Lett. 501 (2001) 92–96.

[35] S.L. Veatch, S.L. Keller, Seeing spots: complex phase behavior in simple membranes, Biochim. Biophys. Acta 1746 (2005) 172–185.

[36] B.Y. van Duyl, D. Ganchev, V. Chupin, B. de Kruijff, J.A. Killian, Sphingomyelin is much more effective than saturated phosphatidylcholine in excluding unsaturated phosphatidylcholine from domains formed with cholesterol, FEBS Lett. 547 (2003) 101–106.

[37] P.-E. Milhiet, M.-C. Giocondi, O. Baghdadi, F. Ronzon, B. Roux, C. Le Grimellec, Spontaneous insertion and partitioning of alkaline phosphatase into model lipid rafts, EMBO Rep. 3 (2002) 485–490.

[38] Y.A. Hannun, Functions of ceramide in coordinating cellular responses to stress, Science 274 (1996) 1855–1859.

[39] R.P. Richter, R. Berat, A.R. Brisson, Formation of solid-supported lipid bilayers: an integrated view, Langmuir 22 (2006) 3497–3505.

[40] J. Shah, J.M. Atienza, R.I. Duclos Jr., A.V. Rawlings, Z. Dong, G.G. Shipley, Structural and thermotropic properties of synthetic C16:0 (palmitoyl) ceramide: effect of hydration, J. Lipid Res. 36 (1995) 1936–1944.

[41] F.M. Goni, A.V. Villar, J.L. Nieva, A. Alonso, Interaction of phospholipases C and sphingomyelinase with liposomes, Methods Enzymol. 372 (2003) 3–19.

[42] B.L. Stottrup, S.L. Veatch, S.L. Keller, Nonequilibrium behavior in supported lipid membranes containing cholesterol, Biophys. J. 86 (2004) 2942–2950.

[43] H.A. Rinia, B. de Kruijff, Imaging domains in model membranes with atomic force microscopy, FEBS Lett. 504 (2001) 194–199.

[44] P.R. Maulik, G.G. Shipley, N-palmitoyl sphingomyelin bilayers: structure and interactions with cholesterol and dipalmitoylphosphatidylcholine, Biochemistry 35 (1996) 8025–8034.

[45] W.-C. Lin, C.D. Blanchette, T.V. Ratto, M.L. Longo, Lipid asymmetry in DLPC/DSPC-supported lipid bilayers: a combined AFM and fluorescence microscopy study, Biophys. J. 90 (2006) 228–237.

[46] A. Choucair, M. Chakrapani, B. Chakravarthy, J. Katsaras, L.J. Johnston, Preferential accumulation of Aβ(1–42) on gel phase domains of lipid bilayers: An AFM and fluorescence study, Biochim. Biophys. Acta 1768 (2007) 146–154.

[47] C.D. Blanchette, W.-C. Lin, T.V. Ratto, M.L. Longo, Galactosylceramide domain microstructure: Impact of cholesterol and nucleation/growth conditions, Biophys. J. 90 (2006) 4466–4478.

[48] D.C. Carrer, S. Schreier, M. Patrito, B. Maggio, Effects of a short chain ceramide on bilayer domain formation, thickness and chain mobility: DMPC and asymmetric ceramide mixtures, Biophys. J. 90 (2006) 2394–2403.

[49] S.L. Veatch, S.L. Keller, Miscibility phase diagrams of giant vesicles containing sphingomyelin, Phys. Rev. Lett. 94 (2005) 148101: 1–4.
[50] J. Sot, L.A. Bagatolli, F.M. Goni, A. Alonso, Detergent-resistant, ceramide-enriched domains in sphingomyelin/ceramide bilayers, Biophys. J. 90 (2006) 903–914.
[51] M.L. Fanani, S. Hartel, R.G. Oliveira, B. Maggio, Bidirectional control of sphingomyelinase activity and surface topography in lipid monolayers, Biophys. J. 83 (2002) 3416–3424.
[52] J.M. Holopainen, M. Subramanian, P.K. Kinnunen, Sphingomyelinase induces lipid microdomain formation in a fluid phosphatidylcholine/sphingomyelin membrane, Biochemistry 37 (1998) 17562–17570.
[53] H.-W. Huang, E.M. Goldberg, R. Zidovetzki, Ceramide induces structural defects into phosphatidylcholine bilayers and activates phospholipase A2, Biochem. Biophys. Res. Commun. 220 (1996) 834–838.
[54] H.-W. Huang, E.M. Goldberg, R. Zidovetzki, Ceramides modulate protein kinase C activity and perturb the structure of phosphatidylcholine/phosphatidylserine bilayers, Biophys. J. 77 (1999) 1489–1497.
[55] J.N. Bai, R.E. Pagano, Measurement of spontaneous transfer and transbilayer movement of BODIPY-labeled lipids in lipid vesicles, Biochemistry 36 (1997) 8840–8848.
[56] H.A. Rinia, R.A. Demel, J.P.J.M. van der Eerden, B. de Krujiff, Blistering of Langmuir–Blodgett bilayers containing anionic phospholipids as observed by atomic force microscopy, Biophys. J. 77 (1999) 1683–1693.
[57] L.R. Cambrea, J.S. Hovis, Formation of three-dimensional structures in supported lipid bilayers, Biophys. J. 92 (2007) 3587–3594.
[58] S. Hartel, M.L. Fanani, B. Maggio, Shape transitions and lattice structuring of ceramide-enriched domains generated by sphingomyelinase in lipid monolayers, Biophys. J. 88 (2005) 287–304.
[59] L.R. Montes, M.B. Ruiz-Arguello, F.M. Goni, A. Alonso, Membrane restructuring via ceramide results in enhanced solute efflux, J. Biol. Chem. 277 (2002) 11788–11794.